

Comparative study of radiation-induced damage in magnesium aluminate spinel by means of IL, CL and RBS/C techniques

Iwona Jozwik¹ · Jacek Jagielski^{1,2} · Grzegorz Gawlik¹ · Przemyslaw Jozwik¹ · Renata Ratajczak² · Gerard Panczer³ · Nathalie Moncoffre⁴ · Anna Wajler¹ · Agata Sidorowicz¹ · Lionel Thomé⁵

Received: 3 November 2015 / Accepted: 11 March 2016 / Published online: 23 March 2016
© The Author(s) 2016. This article is published with open access at Springerlink.com

Abstract A comparative study of damage accumulation in magnesium aluminate spinel (MgAl_2O_4) has been conducted using ionoluminescence (IL), cathodoluminescence (CL) and Rutherford Backscattering Spectrometry/channeling (RBS/C) techniques. MgAl_2O_4 single crystal and polycrystalline samples were irradiated with 320 keV Ar^+ ions at fluencies ranging from 1×10^{12} to 2×10^{16} cm^{-2} in order to create various levels of radiation damage. RBS/C measurements provided quantitative data about damage concentration in the samples. These values were then compared to the luminescence measurements. The results obtained by IL and RBS/C methods demonstrate a two-step character of damage buildup process. The CL data analysis points to the three-step damage accumulation mechanism involving the first defect transformation at fluencies of about 10^{13} cm^{-2} and second at about 10^{15} cm^{-2} . The rate of changes resulting from the formation of non-luminescent recombination centers is clearly nonlinear and cannot be described in terms of continuous accumulation

of point defects. Both, IL and CL techniques, appear as new, complementary tools bringing new possibilities in the damage accumulation studies in single- and polycrystalline materials.

Keywords Magnesium aluminate spinel · Radiation damage · Ionoluminescence · Cathodoluminescence

Introduction

The development of new material expected to be used in a radiative environment requires the solution of numerous problems, one of them being related to the quantitative analysis of radiation disorder in materials. As a first step in material properties assessment, an irradiation with low and high energy ions is frequently used as this method offers numerous advantages; the absence of sample's radioactivity and possibility to get very high damage levels in short times are the main benefits. The problem of information about damage buildup, intensively studied for single crystals by the Rutherford Backscattering Spectrometry/channeling (RBS/C) technique (Tesmer et al. 1995), poses many difficulties for polycrystalline materials. It is especially a serious practical problem, as most of the investigated materials are single crystals, while these are the polycrystals which find the practical application in construction of nuclear reactors.

The aim of the present paper was to use luminescence techniques as an experimental method of quantitative analysis of the radiation damage in polycrystalline materials. The studied case is one of the candidates for inert matrix fuels and alternative waste immobilization matrix, MgAl_2O_4 (Zinkle and Snead 1996; Georgenthum et al. 2001; Pantelica et al. 2005; Schram et al. 2003; Thomé

✉ Iwona Jozwik
iwona.jozwik@itme.edu.pl

¹ Institute of Electronic Materials Technology,
Wolczynska 133, 01-919 Warsaw, Poland

² National Centre for Nuclear Research, Soltana 7,
05-400 Otwock, Swierk, Poland

³ Institut Lumière Matière, UMR5306 Université Lyon
1-CNRS, Université de Lyon, 69622 Villeurbanne Cedex,
France

⁴ Institute de Physique Nucléaire Lyon, UMR5822,
69622 Villeurbanne Cedex, France

⁵ Centre de Spectrométrie Nucléaire et de Spectrométrie
de Masse, IN2P3-CNRS, Université Paris-Sud,
91405 Orsay Cedex, France

et al. 2006; Allen et al. 2010). The use of luminescence techniques is an interesting option, as they may be applied to both, single and polycrystalline solids, are nondestructive, fast and can be easily implemented in situ (Townsend et al. 2007; Skuratov et al. 2006; Jagielski et al. 2014; Gawlik et al. 2011), similar to other techniques, such as XRD (Grygiel et al. 2012).

Experimental

Synthetic single-crystal samples of MgAl_2O_4 (SCI Engineered Materials, Inc.) with a (100) surface and polycrystalline samples obtained at the Institute of Electronic Materials Technology by the hot pressing (Astro, Thermal Technology) of magnesium aluminate nanopowder (Baiowski, La Balme de Sillingy, France) were used in the present study. The samples were organized in three groups: sets N1 and N2 of polycrystalline samples of different grain sizes (56 and 11 μm , respectively) and a set of monocrystalline samples (M).

The specimens were subjected to 320 keV Ar^+ ion irradiations at fluencies ranging from 1×10^{12} to $2 \times 10^{16} \text{ cm}^{-2}$ in order to create various levels of radiation damage. All irradiations were performed at room temperature; the Ar^+ beam power density was kept below 0.1 W/cm^2 to avoid significant heating of samples during irradiation. According to SRIM (Ziegler et al. 1985) calculations, the range of 320 keV Ar^+ ions in MgAl_2O_4 was estimated to be around 200 nm.

The RBS/C measurements were performed using 2.2 MeV $^4\text{He}^{2+}$ ion beam. The RBS/C spectra were fitted using McChasy, a Monte Carlo simulation package allowing the quantitative analysis of channeling spectra (Nowicki et al. 2005). The final outcome of this analysis is the damage accumulation kinetics, i.e., the plots of the damage level versus the irradiation fluence.

The major part of the analysis was devoted to the measure of the luminescence signals generated during the ion or electron irradiation of the spinel crystals. The ionoluminescence signal (IL) was measured using a homemade system based on the use of Hamamatsu spectrometer collecting the light from a sample installed inside a target chamber of an ion implanter (Balzers MPB 202RP) and irradiated with H_2^+ ion beam to excite the luminescence. The H_2^+ ion beam current was kept at the level of 35 μA . The energy and angle of incidence of the H_2^+ —analyzing beam (86 keV at 45 deg) was selected to conform the depth of damage created during the irradiation of the sample with Ar^+ ions of energy 320 keV. Thanks to this approach, the excitation of luminescence of the spinel samples was limited to the damaged layer, avoiding the generation of signal in the unirradiated bulk part. The collection of the IL signal

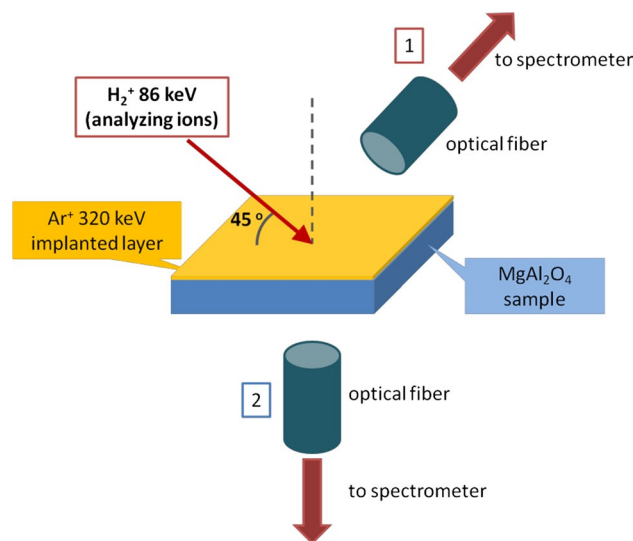


Fig. 1 Schematic drawing of the experimental setup for IL measurements: 1 measurement “at front,” 2 measurement “at back” (not to scale)

was realized with a detector placed either above the Ar -irradiated surface (measurement “at front”) or in the inverse geometry setup (Fig. 1), i.e., behind the specimen (measurement “at back”). The influence of the grain size was analyzed in the present study. For this reason, the samples were also analyzed by electron backscattering diffraction (EBSD) technique in terms of grain size and distribution. The EBSD measurements were performed using Auriga CrossBeam Workstation (Carl Zeiss) equipped with EBSD X-flash detector (Bruker). The 20-keV electron beam of 40 nA probe current was applied for mapping with a pixel size of 0.67 μm .

The CL measurements were performed using a CL system (EM Systems) mounted on Auriga CrossBeam Workstation (Carl Zeiss). The energy of the electron beam was set at 10 keV to sufficiently excite the luminescence signal. According to Casino simulation results (Drouin et al. 2007), in this case, the penetration depth of electrons is approximately 750 nm.

Results and discussion

The set of CL spectra recorded for the set N1 (as an example) are presented in Fig. 2a. For the sake of clarity, the spectra of the virgin sample and first few fluencies are shown. A typical CL spectrum recorded for the magnesium aluminate spinel exhibits two broad bands, the first of which is positioned around 400 nm (consisting in fact of a few emission bands) and demonstrating strong intensity of the luminescence signal. The second band positioned

around 520 nm is much weaker and attributed to Mn^{2+} doping of the $MgAl_2O_4$ (Tomita et al. 2004). The presence of these bands is assigned to transitions from the excited states to lower energy states of the Mn^{2+} ion usually present in the synthetic spinels (Mohler and White 1994). The intensity of both bands rapidly decreases with the irradiation fluence. The IL spectra collected for monocrystalline samples present similar features (Fig. 2b), although the relative intensities of the bands are different from the CL spectra. The emission of ~700 nm band present on both, CL and IL spectra, is assigned to the Cr^{3+} luminescent centers in spinel, where Cr^{3+} appears as a trace constituent substituting Al^{3+} (Gaft et al. 2005).

The values of the intensity of luminescence bands defined as the band area (integrated intensities) were extracted from each spectrum recorded using CL and IL techniques. The IL and CL signals were integrated in the range of 300–350 nm and 462–554 nm, respectively. Subsequently, the integrated intensity of the luminescence signal at a given fluence, I_x , was transformed into reduced values, $I_{x,red}$, defined as:

$$I_{x,red} = (I_0 - I_x)/I_0, \tag{1}$$

where I_0 is the IL or CL signal intensity recorded for unirradiated sample and plotted as functions of the irradiation fluence. This transformation was needed because the intensity of the luminescence signal decreases with the irradiation fluence, whereas the f_D parameter (extracted from RBS/C analysis), which describes the level of radiation damage, increases (Bogh 1968). In order to compare the luminescence and channeling results, it was necessary to transform the luminescence data in the form similar to the RBS/C results. Next, the results of IL, CL and RBS/C analysis were fitted using multistep damage accumulation (MSDA) model (Jagielski and Thomé 2007). That allowed the determination of damage buildup kinetics, and finally cross sections for radiation damage buildup based on the luminescence signal analysis. The values of the MSDA fit parameters based on the IL, CL (taken from Fig. 2) and RBS/C (taken from Fig. 5) data for each set of samples are shown in Tables 1 and 2.

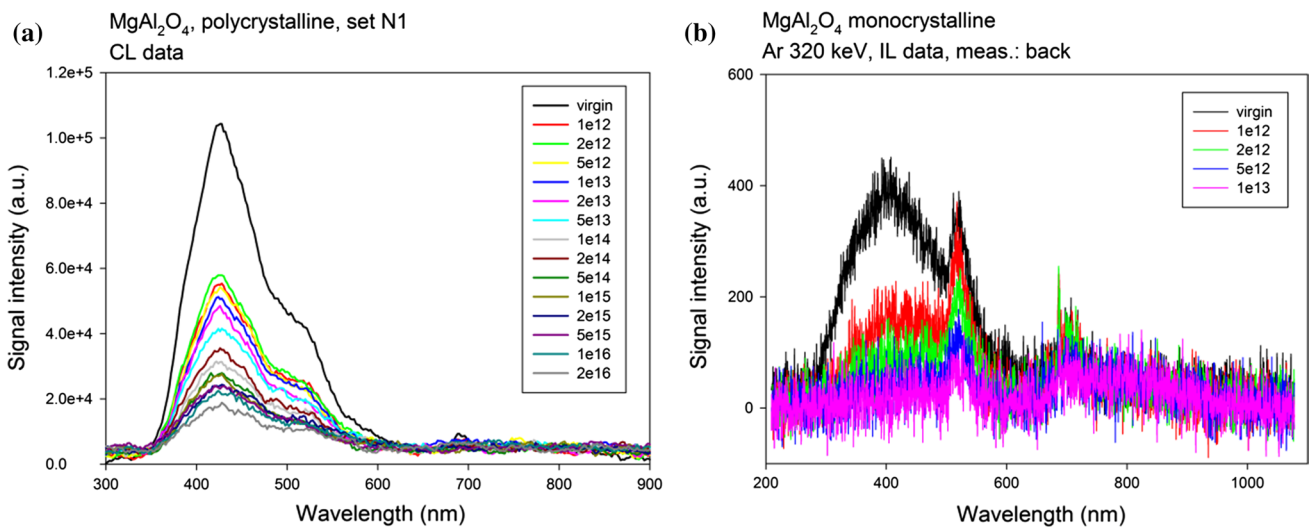


Fig. 2 Luminescence spectra recorded for $MgAl_2O_4$ samples irradiated with Ar^+ ions; **a** CL, polycrystalline samples, **b** IL, single crystals

Table 1 Values of parameters obtained by fitting with the MSDA model for RBS/C and IL data

Parameter (MSDA model)*	Single-crystal RBS/C	Single-crystal IL meas. back	N1 IL meas. back	N1 IL meas. front	N2 IL meas. front
f_{D1}	0.045	0.95	0.913	0.88	0.913
$\sigma_1 [10^{-14} \text{ cm}^2]$	0.4	121	68	209	50
f_{D2}	0.6	1	1	1	1
$\sigma_2 [10^{-14} \text{ cm}^2]$	0.023	15	7	7	4
$\Phi_2 [10^{14} \text{ cm}^{-2}]$	10	0.2	0.1	0.05	0.2

* f_{D1}, f_{D2} damage level at steps 1 and 2; σ_1, σ_2 cross sections for damage accumulation in steps 1 and 2; Φ_2 threshold fluence

Table 2 Values of parameters obtained by fitting with the MSDA model for CL data

Parameter (MSDA model*)	Single crystal CL	N1 CL
f_{D1}	0.59	0.6
σ_1 [10^{-14} cm 2]	60	150
f_{D2}	0.75	0.74
σ_2 [10^{-14} cm 2]	1	2.8
Φ_2 [10^{14} cm $^{-2}$]	0.16	0.15
f_{D3}	0.9	0.8
σ_3 [10^{-14} cm 2]	0.03	0.03
Φ_3 [10^{14} cm $^{-2}$]	19	50

* f_{D1} , f_{D2} , f_{D3} damage level at steps 1, 2 and 3; σ_1 , σ_2 , σ_3 cross sections for damage accumulation in steps 1, 2 and 3; Φ_2 , Φ_3 threshold fluencies

Analysis of the IL data

The samples from the sets N1 and N2 were analyzed in terms of the influence of the grain size on the damage accumulation kinetics based on the IL response. Additionally, two techniques of the signal collection were tested: signal measured “at front,” i.e., when the detector placed over the sample surface, and “at back,” when the optical fiber guiding the emitted light to the spectrometer was placed at the back side of the sample. This was realized in the following manner: samples N1: measured either “at front” and “at back,” samples N2: measured “at front,” samples M: measured “at back.” The technique to measure the IL signal “at back” is useful in case of transparent samples and allows to avoid the influence of the carbon layer appearing on the sample surface in the result of implantation.

The influence of the grain size on the IL signal (sets N1 and N2)

Figure 3 presents the results of the analysis of the IL signal measured “at front” for two sets of polycrystalline samples, N1 and N2, along with the MSDA fits. In the case of both sets of the samples, the changes of the reduced intensity of the IL signal with irradiation fluence exhibit a two-step character, although step 2 represents approximately 10 % of the signal [step 1 reaching ~0.9 (see Table 1)]. The threshold value of the Ar $^+$ -irradiation fluence is larger by the factor of 4 for the set N2 in comparison with the set N1, reaching 0.2×10^{-14} and 0.05×10^{-14} cm $^{-2}$, respectively.

The observed differences are most likely related to the different grain sizes in the samples of set N1 comparing to N2, which were 56 and 11 μ m, respectively. Of course, in samples with smaller grains (N2), concentration of grain boundaries is much higher than in samples with large grains (N1). Taking into account that the grain boundaries

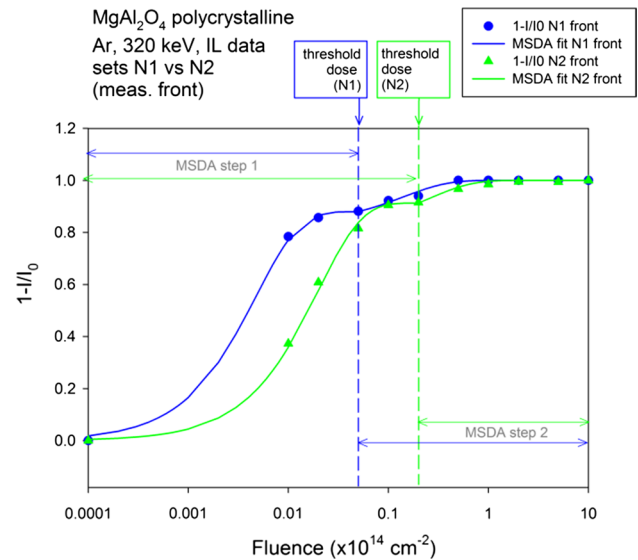


Fig. 3 The dependencies of reduced intensity of IL signal values on the irradiation fluence (damage kinetics) for polycrystalline MgAl $_2$ O $_4$ samples irradiated with 320 keV Ar $^+$ ions

work like “sinks” for the irradiation defects, the origin of a shift in the threshold fluence between the sample N1 and N2 becomes obvious. The defect-depletion regions can be formed along the grain boundaries, so that the sample with smaller grains remains less damaged in the result of the same irradiation fluence. In other words, the irradiation fluence must be higher in order to create the same level of damage and trigger the structural transformation in the sample with smaller grains.

Polycrystalline versus monocrystalline samples (IL data, sets N1 and M)

Thanks to the proper selection of the ion energy used for the analysis, it was possible to avoid IL signal generation in unmodified parts of the samples. The reduced value of IL signal mimics the behavior of the f_D parameter, i.e., it is equal to 0 for unirradiated sample and 1 for the sample with no luminescence signal recorded (Fig. 4).

In the case studied, the two-step behavior of the changes of IL signal was observed and the complete decay of the IL intensity at the fluence of Ar $^+$ ions equal to 1×10^{14} cm $^{-2}$. Practically, the same threshold fluences were observed for samples sets N1 and M, (about 1×10^{13} and 2×10^{13} cm $^{-2}$, respectively). Slightly faster damage accumulation in single crystals in low fluence range (1×10^{12} – 1×10^{13} cm $^{-2}$) most likely can be explained by higher stress level in single crystals. The role of grain boundaries cannot be completely ruled out; however, their influence on defect evolution in a material composed of grains having the size of more than 50 micrometers when the irradiated layer is only

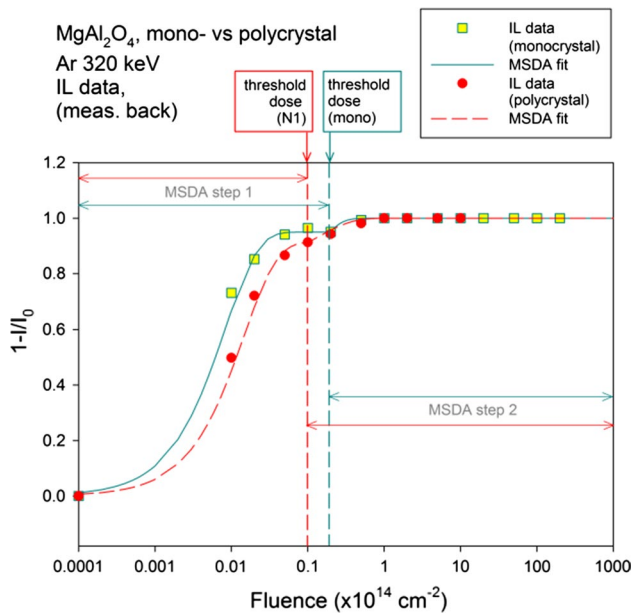


Fig. 4 The dependencies of reduced intensity of IL signal values on the irradiation fluence (damage kinetics) for mono- and polycrystalline MgAl_2O_4 samples irradiated with 320 keV Ar^+ ions

0.2 micrometers thick should rather be minor, as the sample volume affected by grain boundaries is very small in material composed of very large grains. The character of the IL signal decrease (or increase in the reduced IL signal) is very similar in the case of single- and polycrystalline spinel samples. This confirms the ionoluminescence technique as the proper investigation tool, which may be used for comparative analysis of radiation damage in single- and polycrystals.

Analysis of CL data for the sets N1 and M

The CL data analyzed in terms of reduced signal intensity and fitted with MSDA model exhibited three-step behavior of damage accumulation process. The first threshold was observed for the Ar^+ fluence of 0.15×10^{14} and $0.16 \times 10^{14} \text{ cm}^{-2}$ for N1 and M samples, respectively. The second transformation could be observed at $5 \times 10^{15} \text{ cm}^{-2}$ for N1 and $1.9 \times 10^{15} \text{ cm}^{-2}$ for M samples. The summary of the fit parameters is presented in Table 2. It seems that the CL technique is sensitive to the structural changes in the material at very early stages even in comparison with IL technique.

Comparison of RBS/C, IL and CL data for the set M

The results of analysis for monocrystalline samples obtained by three different techniques (IL, CL and RBS/C) are summarized in Fig. 5. Both IL and RBS/C techniques exhibit the two-step behavior of the damage kinetics.

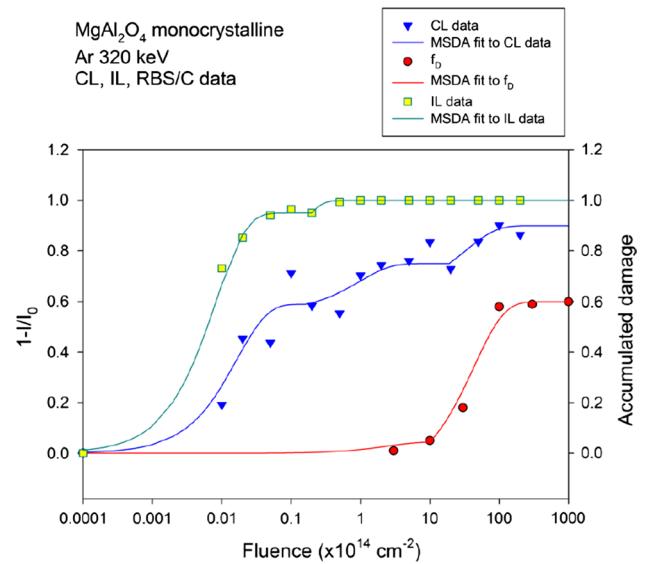


Fig. 5 Damage accumulation kinetics calculated from: RBS/C data (circles), IL data (squares) and CL data (triangles); all dependencies fitted with the MSDA model

However, the threshold value of the irradiation fluence in the case of IL signal is different from the RBS/C result (2×10^{13} vs. $1 \times 10^{15} \text{ cm}^{-2}$, respectively).

The CL technique seems to bring more insight into the damage accumulation process comparing with the IL and RBS/C. The results of CL exhibit the three-step mechanism of defect transformation in the irradiated spinel. Noteworthy is the fact that first stage of transformation occurs at a similar threshold fluence as for the IL data (0.45×10^{14} vs. $0.2 \times 10^{14} \text{ cm}^{-2}$), while the second one is close to the value calculated based on RBS/C results (1.9×10^{15} vs. $1 \times 10^{15} \text{ cm}^{-2}$). This demonstrates that CL and IL are techniques sensitive to the early stages of damage production in comparison with RBS/C.

Summary and conclusions

The response of the magnesium aluminate spinel samples investigated by means of IL and CL techniques seems to be governed by different phenomena than in the case of RBS/C method. The luminescence signal decreases rapidly at very low radiation fluencies, when the changes in the f_D parameter are rather small (Fig. 4). The mechanism of such a fast decay of IL signal is not known yet, but it seems that it mostly relies on the formation of nonradiative recombination centers as a result of creation of vacancies by Ar^+ ions. Thus, the luminescence may disappear already at the early stages of irradiation without altering the f_D parameter which is sensitive mainly to the concentration of interstitial atoms displaced from their original positions and is almost

completely insensitive to vacancies (Jagielski et al. 2014). As the significant increase of the values of f_D is related to the transformation of defects from small defect clusters into dislocations or dislocation loops (Jagielski and Thomé 2009, 2011), such a transformation is observed at relatively high irradiation fluencies.

In the case when the analysis of damage was based on the CL measurements, the recorded signal never faded completely, as its generation occurs well beneath the damaged layer of the investigated sample. This is due to relatively high electron beam-accelerating voltage and resulting electron penetration depth, which is approximately 750 nm for 10-keV electron beam in $MgAl_2O_4$ (Drouin et al. 2007). Nevertheless, the technique seems to be complementary to IL and RBS/C. Both IL and CL techniques appear more sensitive than RBS/C in a low fluence range. The results obtained confirm also the potential of luminescence techniques for studies of damage accumulation by the comparison of the kinetics of luminescence signal (reduced signal intensity vs. irradiation fluence) with the results of the RBS/C experiments.

The analysis of light emitted from the sample excited with charged energetic particles may provide useful information on the damage accumulation in an irradiated material, as shown above. Both IL and CL appear thus as suitable tools for the analysis of the damage accumulation kinetics. However, the rate of changes resulting from the formation of nonluminescent recombination centers is very different than that resulting from the creation of single defect clusters or dislocations. It means that the phenomena responsible for the decrease of the luminescence are different than those related to the creation of displaced atoms present in the crystal channels. Consequently, IL and CL techniques may be considered as complementary tools showing new perspectives in the damage accumulation studies in single- and polycrystalline materials. Another advantage of the ionoluminescence technique is that it may be implemented also “in situ” in various equipments such as ion implanters and tandem accelerators. The experiments are fast, relatively easy, inexpensive and offer a unique possibility to use the same ion beam for both the creation and the simultaneous analysis of radiation damage.

Acknowledgments This work was partially sponsored by the National Science Centre (Poland) under the Contract Number DEC-2011/03/D/ST8/04490 and by 09-133 French—Polish collaboration program.

Open Access This article is distributed under the terms of the Creative Commons Attribution 4.0 International License (<http://creativecommons.org/licenses/by/4.0/>), which permits unrestricted use, distribution, and reproduction in any medium, provided you give appropriate credit to the original author(s) and the source, provide a link to the Creative Commons license, and indicate if changes were made.

References

- Allen T, Busby J, Meyer M, Petti D (2010) Materials challenges for nuclear systems. *Mater Today* 13(12):14–23. doi:10.1016/S1369-7021(10)70220-0
- Bogh E (1968) Defect studies in crystals by means of channeling. *Can J Phys* 46:653–662. doi:10.1139/p68-081
- Drouin D, Couture AR, Joly D, Tastet X, Aimez V, Gauvin R (2007) CASINO V2.42—a fast and easy-to-use modeling tool for scanning electron microscopy and microanalysis users. *Scanning* 29:92–101. doi:10.1002/sca.20000
- Gaft M, Reisfeld R, Panczer G (2005) Modern luminescence spectroscopy of minerals and materials. Springer, Berlin
- Gawlik G, Sarnecki J, Jozwik I, Jagielski J, Pawłowska M (2011) Ion and electron beam induced luminescence of rare earth doped YAG crystals. *Acta Phys Polonica A* 120:181–183
- Georgenthum V, Brillaud J, Chauvin N, Pelletier M, Noirot J, Plancq D (2001) Experimental study and modelling of the thermoelastic behaviour of composite fuel in reactors—emphasis on spinel based composites. *Prog Nucl Energy* 38:317–320. doi:10.1016/S0149-1970(00)00125-6
- Grygiel C, Lebius H, Bouffard S, Quentin A, Ramillon J M, Madi T, Guillou S, Been T, Guinement P, Lelièvre D, Monnet I (2012) Online *in situ* x-ray diffraction setup for structural modification studies during swift heavy ion irradiation. *Rev Sci Instrum* 83:013902(1–6). doi:10.1063/1.3680106
- Jagielski J, Thomé L (2007) Damage accumulation in ion-irradiated ceramics. *Vacuum* 81:1352–1356. doi:10.1016/j.vacuum.2007.01.059
- Jagielski J, Thomé L (2009) Multi-step damage accumulation in irradiated crystals. *Appl Phys A* 97:147–155. doi:10.1007/s00339-009-5294-z
- Jagielski J, Thomé L (2011) Discontinuous character of the damage build-up in the elastic collision regime. *Rad Eff Def Solids* 166:367–372. doi:10.1080/10420150.2011.556117
- Jagielski J, Gawlik G, Jozwik-Biala I, Panczer G, Moncoffre N, Wang X, Ratajczak R, Swirkowicz M, Thomé L (2014) Luminescence analysis of damage accumulation; case study of calcium molybdate. *Nucl Instr Meth Phys Res B* 332:60–62. doi:10.1016/j.nimb.2014.02.030
- Mohler RL, White WB (1994) Influence of structural order on the luminescence of oxide spinels: manganese activated spinels. *Mat Res Bull* 29(10):1109–1116. doi:10.1016/0025-5408(94)90094-9
- Nowicki L, Turos A, Ratajczak R, Stonert A, Garrido F (2005) Modern analysis of ion channeling data by Monte Carlo simulations. *Nucl Instr Meth Phys Res B* 240:277–282. doi:10.1016/j.nimb.2005.06.129
- Pantelica D, Ionescu P, Negoita F, Scintee N, Thomé L, Enescu SE, Jagielski J (2005) Complementary use of ERDA and RBS/C for the determination of implanted atom and damage distributions in spinel. *Nucl Instr Meth Phys Res B* 240:376–380. doi:10.1016/j.nimb.2005.06.163
- Schram RPC, van der Laan RR, Klaassen FC, Bakker K, Yamashita T, Ingold F (2003) The fabrication and irradiation of plutonium-containing inert matrix fuels for the ‘Once Though Then Out’ experiment. *J Nucl Mater* 319:118–125. doi:10.1016/S0022-3115(03)00143-0
- Skuratov VA, Gun KJ, Stano J, Zagorski DL (2006) In situ luminescence as monitor of radiation damage under swift heavy ion irradiation. *Nucl Instr Meth Phys Res B* 245:194–200. doi:10.1016/j.nimb.2005.11.100
- Tesmer JR, Nastasi M, Maggiore CJ, Barbour JC, Mayer JW (1995) Handbook of modern ion beam materials analysis. Materials Research Society, Pittsburgh, PA

- Thomé L, Gentils A, Jagielski J, Garrido F, Thomé T (2006) Physico-chemical modifications induced by ion bombardment and thermal treatments in zirconia and spinel. *Nucl Instr Meth Phys Res B* 250:106–113. doi:[10.1016/j.nimb.2006.04.147](https://doi.org/10.1016/j.nimb.2006.04.147)
- Tomita A, Sato T, Tanaka K, Kawabe Y, Shirai M, Tanaka K, Hanamura E (2004) Luminescence channels of manganese-doped spinel. *J Lumin* 109:19–24. doi:[10.1016/j.jlumin.2003.12.049](https://doi.org/10.1016/j.jlumin.2003.12.049)
- Townsend PD, Khanlary M, Hole DE (2007) Information obtainable from ion beam luminescence. *Surf Coat Technol* 201:8160–8164. doi:[10.1016/j.surfcoat.2006.01.075](https://doi.org/10.1016/j.surfcoat.2006.01.075)
- Ziegler JF, Biersack JP, Littmark U (1985) *The stopping and range of ions in solids*. Pergamon, New York
- Zinkle SJ, Snead LL (1996) Influence of irradiation spectrum and implanted ions on the amorphization of ceramics. *Nucl Instr Meth Phys Res B* 116:92–101. doi:[10.1016/0168-583X\(96\)00016-X](https://doi.org/10.1016/0168-583X(96)00016-X)